

# Semiclassical approach to the density of states of the disordered electron gas in a quantum wire

Doan Nhat Quang

*Center for Theoretical Physics, National Center for Natural Science and Technology, P.O. Box 429 Boho, Hanoi 10000, Vietnam*

Nguyen Huyen Tung

*Institute of Engineering Physics, Hanoi University of Technology, 1 Dai Co Viet Road, Hanoi, Vietnam*

(Received 23 December 1998)

A theory is given of the density of states (DOS) of the quasi-one-dimensional electron gas (1DEG) in a semiconductor quantum wire in the presence of some random field. For a smooth random field, the derivation is carried out within Gaussian statistics and a semiclassical model. The DOS is then obtained in a simple analytic form, where the input function for disorder interaction is the autocorrelation function of the random field. This allows one to take completely into account the geometry of the wire, the origin of disorder, and the many-body screening by 1D electrons. The DOS is demonstrated to be composed of the classical DOS and the quantum correction, which are connected with fluctuations in the random potential and in the random force, respectively. The disorder is found to smear out the square-root singularity of the DOS of the ideal 1DEG into a finite peak tailing below the subband edge. The disorder effects from impurity doping and surface roughness on the DOS of the 1DEG in a cylindrical GaAs wire of radius  $R$  are thoroughly examined. It is shown that for  $R \leq a^*/2$  (with  $a^*$  as the effective Bohr radius) surface roughness with a radius fluctuation equal to 10% of  $R$  overwhelms impurity doping with a density  $n_i = 10^6 \text{ cm}^{-3}$ , but for  $R \geq 2a^*$  the latter is dominant.

[S0163-1829(99)02940-9]

## I. INTRODUCTION

In recent years, quantum wire (QWR) structures have attracted much attention, and promising advances have been obtained in fabrication and application of QWR's, e.g., laser devices.<sup>1</sup> This is primarily motivated by their unique transport properties, viz., high electronic mobility<sup>2</sup> as well as the expected enhanced optical properties such as high differential optical gain<sup>3</sup> and optical nonlinearities.<sup>4</sup> Thus, from both fundamental and applied physics viewpoints, there has been a growing interest in understanding the electronic properties of QWR's.

It is well known that various QWR's may be adequately described in terms of a quasi-one-dimensional electron gas, hereafter called for short a one-dimensional electron gas (1DEG), where the electron dynamics is essentially restricted to be one dimensional. In practice, 1DEG's are always affected by disorder caused by some random field present in QWR's. The field is of different origins, e.g., impurity doping,<sup>5-8</sup> surface roughness,<sup>5-10</sup> and alloy disorder.<sup>5,7,11</sup> The disorder has been shown to lead to considerable changes in the electronic energy spectrum of the 1DEG, e.g., destroying the square-root singularity of the density of states (DOS) characteristic of an ideal 1DEG.<sup>12,13</sup> Moreover, the disorder also gives rise to an appreciable modification in the elementary collective-excitation spectrum of the 1DEG, e.g., the dispersion for long-wavelength plasmons.<sup>14</sup> Obviously, these in turn result in remarkable changes in many phenomena occurring in the wire, e.g., optical absorption. Therefore, having useful (especially analytic) expressions for the DOS's of disordered 1DEG's is of fundamental importance in both explaining observable properties of QWR's and analyzing the performance of modern semiconductor devices based on them.

So far, only a few theoretical investigations<sup>12,13,15,16</sup> have been made in order to understand the electronic energy spectrum of disordered 1DEG's in QWR's, and only numerical results have been available in the literature. It should be surprisingly noted that the existing theories of the effect of disorder on the 1D DOS have been established only for the disorder arising from charged impurities chaotically distributed in the sample. The other sources of disorder, especially surface roughness, have recently been confirmed experimentally to be of importance in very thin QWR's.<sup>17-19</sup> Nevertheless, the consideration of their influence on the 1D DOS has seemingly been quite scarce. The reason for this is probably that in the earlier theories the input function for disorder interaction has been chosen to be the potential created by an individual center of force, e.g., a single ionized impurity in doped QWR's. The one-center potential is clearly inadequate for describing disorder interaction connected, e.g., with surface roughness.

Furthermore, existing theories of the impurity doping effect turn out to be partly unsatisfactory. Indeed, Das Sarma and Xie<sup>15</sup> calculated the DOS for a 1DEG in a doped rectangular QWR. The calculation is based on a self-consistent Born approximation and, hence, is adequate mainly for a low doping level. Takeshima<sup>12</sup> evaluated the 1D DOS for a heavily doped square wire, employing the semiclassical model suggested by Kane<sup>20</sup> and Bonch-Bruевич<sup>21</sup> for 3D electron systems. However, a serious shortcoming of this theory is the use of a 3D (bulklike) screened Coulomb impurity potential, which is evidently seen to dramatically overestimate the screening by 1D electrons since the 1D electron system may be polarized merely along the wire axis.<sup>22</sup> Therefore, the authors of Ref. 13 applied Klaunder's best multiple-scattering approach<sup>23</sup> to evaluating the 1D DOS in a doped cylindrical wire. This enables us to allow for

the geometry of the wire and the features of the many-body interaction in the IDEG, e.g., 1D screening of the impurity field. However, the method must invoke drastic approximations, and despite these it is computationally still very complicated for realistic IDEG's. Further, the authors of Ref. 16 used a 1D version of the multiple-scattering theory of Matsubara and Toyozawa.<sup>24</sup> Nevertheless, this is essentially a single-band scheme and, hence, can describe the impurity band formation rather than the tailing of the 1D DOS.

Thus the goal of the present paper is to develop a theory of the electronic energy spectrum of disordered IDEG's in QWR's, which is to be applicable to disorder not only arising from impurity doping but also of any origins relevant to realistic QWR structures, and which must eliminate the above-mentioned difficulties of the existing theories. To this end, we will propose a version of the semiclassical approach to IDEG's subjected to smooth random fields, based on modifying the method suggested by Quang and Tung<sup>25</sup> for 2D electron systems. This version allows taking complete account of the microscopic details of the geometry of the wire and the origin of the disorder, and providing the DOS of disordered IDEG's in a simple analytic form.

In Sec. II, we start with a collection of the formulas to be used for calculating the DOS of the IDEG in the presence of some Gaussian random field. The derivation of the DOS of disordered IDEG's in smooth Gaussian fields proceeds in Sec. III within a semiclassical approach. This accounts for the classical effect due to fluctuations in the random potential as well as the quantum effect due to fluctuations in the random force. In Sec. IV, the theory is applied to a cylindrical wire where the disorder is produced by both impurity doping and surface roughness. In Sec. V, illustrating plots and conclusions are presented. Finally, Sec. VI is devoted to a summary.

## II. BASIC RELATIONS

Two striking aspects of strictly 1D electron systems have been shown theoretically. For noninteracting electrons in the presence of any disorder, all electronic states are exponentially Anderson localized.<sup>26</sup> On the other hand, within the Tomonaga-Luttinger model for interacting electrons (linear electron energy dispersion, infinite density of negative-energy electrons, and short-range interaction), the electrons in a single-subband QWR in the absence of disorder make up a singular strongly correlated liquid.<sup>27</sup> Thus the disordered interacting strictly IDEG was believed, in principle, to behave as a localized, strongly correlated Luttinger liquid.

Contrary to the above long-standing theoretical claim, Das Sarma and co-workers<sup>28-30</sup> recently proved, based on a more realistic model (parabolic dispersion, finite electron density, and Coulomb interaction), that even a small amount of disorder in an interacting IDEG would restore the Fermi surface if the localization length becomes larger than the physical length of the wire. The typical localization lengths turn out to be very long (larger than 10–100  $\mu\text{m}$ ).<sup>31</sup> Therefore, IDEG's in QWR's with both disorder and electron-electron interactions behave, for all practical purposes, essentially as delocalized Fermi liquids.<sup>28-31</sup> There has been an

abundance of recent experiments which offer clear evidence supporting the standard Fermi-liquid model for actual IDEG's.<sup>32-37</sup> Until now, all theories of disordered interacting IDEG's, e.g., in semiconductor QWR's<sup>5-8,12-16,28-31,38,39</sup> and graphene nanotubes,<sup>40-42</sup> have seemed to be developed within this model. These were found to be quantitatively highly successful in explaining the experimental data on the electronic properties of realistic QWR's, e.g., Raman scattering, photoluminescence, and band-gap renormalization.

Thus in what follows we may ignore all aspects of localization and Luttinger-liquid physics uncritically, starting from the standard Fermi-liquid model. The electrons in the wire are considered to be confined in two dimensions, e.g., in the  $y$  and  $z$  directions, and to move freely in the  $x$  direction (chosen as the wire axis). The disorder in the wire is usually caused by some random field affecting the motion of the electrons along the wire axis.

Hereafter, we shall restrict the discussion to the case when the random field  $U(x)$  obeys Gaussian statistics. Therefore, it may completely be described by the autocorrelation function of the disorder potential

$$W(x-x') = \langle U(x)U(x') \rangle, \quad (1)$$

where the angular brackets stand for averaging over all configurations of the random field. The disordered electron system is assumed macroscopically homogeneous, the autocorrelation function depending merely on the coordinate difference.

As usual, the strength of the field is determined by the rms of its potential  $\gamma$  and of its force  $F$ , defined by

$$\gamma^2 = \langle U^2 \rangle = W(x-x')|_{x=x'}, \quad (2)$$

and

$$F^2 = \langle (\nabla U)^2 \rangle = \nabla_x \nabla_{x'} W(x-x')|_{x=x'}. \quad (3)$$

The average potential is supposed small compared with the energy separation between neighboring subbands, so that the intersubband scattering induced by disorder is negligible and the theory may be formulated in a one-subband approximation.

It is well known<sup>43</sup> that the DOS is the most adequate concept describing the energy spectrum of disordered systems. The electronic DOS per unit length can be represented in terms of a Fourier transform of the Green's function as

$$\rho(E) = \frac{1}{\pi\hbar} \int_{-\infty}^{\infty} dt \exp(iEt/\hbar) \langle G(t) \rangle, \quad (4)$$

where a spin degeneracy of 2 is included. Here  $\langle G(t) \rangle$  denotes the diagonal part of the configuration-averaged Green's function, which describes the one-particle properties of the IDEG in the presence of a random field and is clearly independent of the spatial coordinate in virtue of the macroscopic homogeneity of the electron system.

The Green's function may be written within the one-subband approximation in terms of a Feynman path integral as<sup>43</sup>

$$G(t) = \left( \frac{m}{2\pi i \hbar t} \right)^{1/2} \frac{1}{\mathcal{N}} \oint \mathcal{D}x(\tau) \exp \left\{ \frac{i}{\hbar} \int_0^t d\tau \right. \\ \left. \times \left[ \frac{m}{2} \dot{x}^2(\tau) - U[x(\tau)] \right] \right\}. \quad (5)$$

Here  $m$  is the effective mass of the charge carriers with a parabolic 1D subband reckoned from the unperturbed subband edge,  $\mathcal{D}x(\tau)$  means the Feynman measure, and  $\mathcal{N}$  is the normalization factor:

$$\mathcal{N} = \oint \mathcal{D}x(\tau) \exp \left\{ \frac{i}{\hbar} \int_0^t d\tau \frac{m}{2} \dot{x}^2(\tau) \right\}. \quad (6)$$

The path integrals in Eqs. (5) and (6) are taken over closed paths:  $x(t) = x(0)$ .

For a Gaussian random field, it holds for the averaged Green's function<sup>43</sup> that

$$\langle G(t) \rangle = \left( \frac{m}{2\pi i \hbar t} \right)^{1/2} \frac{1}{\mathcal{N}} \oint \mathcal{D}x(\tau) \exp \left\{ \frac{i}{\hbar} \int_0^t d\tau \frac{m}{2} \dot{x}^2(\tau) \right. \\ \left. - \frac{1}{2\hbar^2} \int_0^t d\tau \int_0^t d\tau' W[x(\tau) - x(\tau')] \right\}. \quad (7)$$

Thus Eqs. (4) and (7) set up a basis for studying the DOS of the IDEG in a QWR in the presence of a Gaussian random field. The disorder effect is then allowed for via the autocorrelation function, whose form is specified by the geometry of the wire and the nature of the disorder.<sup>5-8</sup>

### III. DOS OF DISORDERED IDEG'S IN A SEMICLASSICAL MODEL

For further evaluation of the DOS of disordered IDEG's, we have to calculate the averaged Green's function provided by Eq. (7). Hereafter we will assume that the random field  $U(x)$  producing disorder in the electron system obeys the inequality

$$\frac{\hbar^2 F^2}{4m\gamma^3} \ll 1, \quad (8)$$

where  $\gamma$  and  $F$  are, as before, the averages of the random potential and of the random force, given by Eqs. (2) and (3).

It has been pointed out<sup>44,45</sup> that if inequality (8) is fulfilled, the field  $U(x)$  and, hence, its autocorrelation function  $W(x-x')$ , are varying slowly on the average along the wire axis, so that a semiclassical approach to it may be applicable. As a consequence, the Green's function (7) is to be approximated in the lowest order by<sup>25,46</sup>

$$\langle G(t) \rangle = \left( \frac{m}{2\pi i \hbar t} \right)^{1/2} \exp \left( - \frac{\gamma^2 t^2}{2\hbar^2} \right) \left[ 1 + \frac{\gamma^2 t^2 - J(t)}{2\hbar^2} \right], \quad (9)$$

where  $J(t)$  is a path integral, defined by

$$J(t) = \frac{1}{\mathcal{N}} \oint \mathcal{D}x(\tau) \exp \left\{ \frac{i}{\hbar} \int_0^t d\tau \frac{m}{2} \dot{x}^2(\tau) \right\} \\ \times \int_0^t d\tau \int_0^t d\tau' W[x(\tau) - x(\tau')]. \quad (10)$$

It is to be noticed that the first and second terms inside the square brackets on the right-hand side of Eq. (9) are responsible for the classical DOS in the subband-bending model and the quantum correction relative to fluctuations in the random force, respectively.

Now, we must evaluate the function  $J(t)$  entering Eq. (9). The evaluation of the integrals present in Eq. (10) is outlined as follows. First the autocorrelation function in Eq. (10) is to be replaced by its Fourier transform with  $\mathbf{k}$  as a 1D wave vector, defined by

$$W(x) = \int_{-\infty}^{\infty} \frac{d\mathbf{k}}{2\pi} W(\mathbf{k}) \exp(i\mathbf{k}x). \quad (11)$$

Then the path integral is straightforward, yielding<sup>25</sup>

$$J(t) = \int_{-\infty}^{\infty} \frac{d\mathbf{k}}{2\pi} W(\mathbf{k}) \int_0^t d\tau \int_0^t d\tau' \exp \left[ -i \frac{\hbar k^2 t}{2m} \sigma(1-\sigma) \right], \quad (12)$$

where  $\sigma = |\tau - \tau'|/t \leq 1$  and  $k = |\mathbf{k}|$ .

Next, it is evidently seen from Eqs. (4) and (9) that the main contribution to the semiclassical DOS results from such a time region that

$$\gamma t / \hbar \leq 1, \quad (13)$$

with  $\gamma$  being the average random potential.

Furthermore, the  $\mathbf{k}$  integral in the Fourier representation (11) of the autocorrelation function is primarily extended over such a wave-vector region that

$$k \leq 1/L. \quad (14)$$

Here  $L$  is a correlation length of the random field that the function  $W(x)$  becomes small under  $|x| \geq L$ , the field fluctuations with a spacing larger than  $L$  being statistically independent.

Upon combining inequalities (13) and (14), we are in a position to estimate the upper limit of the variable of the exponential in Eq. (12):

$$\frac{\hbar k^2 t}{m} \lesssim \frac{\hbar^2 / mL^2}{\gamma}. \quad (15)$$

In accordance with the semiclassical nature of the random field, we may, as usual, adopt the following inequality:

$$\frac{\hbar^2 / mL^2}{\gamma} \ll 1. \quad (16)$$

Then expanding the exponential in Eq. (12) into a series in powers of the small quantity  $\hbar k^2 t / m$ , the function  $J(t)$  is to be approximated in the lowest order by

$$J(t) = \gamma^2 t^2 + \frac{\hbar F^2}{12m} (it)^3. \quad (17)$$

The rms of the potential and of the force of the random field figuring in Eq. (17) can now be rewritten in terms of the Fourier transform of the autocorrelation function as

$$\gamma^2 = \int_{-\infty}^{\infty} \frac{d\mathbf{k}}{2\pi} W(\mathbf{k}) \quad (18)$$

and

$$F^2 = \int_{-\infty}^{\infty} \frac{d\mathbf{k}}{2\pi} \mathbf{k}^2 W(\mathbf{k}). \quad (19)$$

Finally, on substitution of the function  $J(t)$  in Eq. (9) by Eq. (17), we may immediately arrive at the following averaged Green's function describing the 1DEG moving in a smooth Gaussian field:

$$\langle G(t) \rangle = \left( \frac{m}{2\pi i \hbar t} \right)^{1/2} \exp\left(-\frac{\gamma^2 t^2}{2\hbar^2}\right) \left[ 1 - \frac{F^2}{24\hbar m} (it)^3 \right], \quad (20)$$

Let us now return to the derivation of the DOS for the 1DEG in question. We need to insert the Green's function (20) into Eq. (4), and perform easily the appearing  $t$  integral by means of<sup>47</sup>

$$\begin{aligned} & \int_{-\infty}^{\infty} dx (ix)^\nu \exp(-\beta^2 x^2 - iqx) \\ &= \frac{\sqrt{\pi}}{2^{\nu/2} \beta^{\nu+1}} \exp\left(-\frac{q^2}{8\beta^2}\right) D_\nu\left(\frac{q}{\beta\sqrt{2}}\right), \end{aligned} \quad (21)$$

with  $D_\nu(x)$  being a parabolic cylinder function. As a consequence, we obtain

$$\begin{aligned} \rho(E) &= \frac{1}{\pi} \left( \frac{2m}{\hbar^2} \right)^{1/2} \frac{1}{(2\gamma)^{1/2}} \exp\left(-\frac{E^2}{4\gamma^2}\right) \\ &\times \left[ D_{-1/2}\left(-\frac{E}{\gamma}\right) - \frac{\hbar^2 F^2}{24m\gamma^3} D_{5/2}\left(-\frac{E}{\gamma}\right) \right]. \end{aligned} \quad (22)$$

Thus, within the semiclassical model, the DOS of disordered 1DEG's in QWR's is provided by Eqs. (22), (18), and (19). This general analytic form of the 1D DOS is the central result of the present paper.

With the aid of the asymptotic expansion of the parabolic cylinder function,<sup>47</sup> it follows immediately from Eq. (22) that if the disorder is absent the semiclassical DOS can reproduce the square-root singularity at the subband edge, characteristic of the ideal 1DEG,<sup>1</sup>

$$\rho_0(E) = \frac{1}{\pi} \left( \frac{2m}{\hbar^2} \right)^{1/2} \frac{\theta(E)}{E^{1/2}}, \quad (23)$$

where  $\theta(t)$  is the Heaviside step function.

In analogy with disordered 2D electron systems,<sup>25</sup> within the semiclassical approach to a smooth Gaussian field the DOS of disordered 1D electron systems may, as expected, be represented in terms of an expansion with respect to the small quantity  $\hbar^2 F^2 / 4m\gamma^3$ . It is obvious that the first term inside the square brackets on the right-hand side of Eq. (22) refers to the classical DOS, while the second one to the quantum correction. The former depends merely on the rms of

fluctuations in the potential of the random field,  $\gamma$ , whereas the latter depends not only on the rms of fluctuations in its potential  $\gamma$  but in its force  $F$  as well.

It is interesting to note that our approach to a random field is capable of including the disorder effect from the potential and its first spatial derivative into the DOS calculation, while the purely classical approximation of Kane<sup>20</sup> includes that from the potential only, and the quantum method of Halperin and Lax<sup>43</sup> that from the potential as well as its first and second derivatives.

It should be stressed that the semiclassical approach has assumed the random field to be smooth, which implies, as seen below a large width of the wire, a high doping level, and small fluctuations in the wire width. The smoothness condition (8) involves only long-range fluctuations in the disorder potential, and corresponds to the short-time case specified by inequality (13). Consequently, the theory may describe properly the high-energy region above and near the subband edge (the latter is of the order of the rms potential). This may be understood physically by considering the Heisenberg energy-time uncertainty relation in combination with inequality (13).

It is worthy to note that because of its simple form, our approach is a flexible tool for the theoretical investigation of disorder effects on the DOS of 1DEG's in semiconductor QWR's. It follows from Eqs. (22), (18), and (19) that in distinction from the existing theories,<sup>12-16</sup> rather than the potential due to a single center of force but the autocorrelation function of the random field plays the key role as the input function for disorder interaction. In the most discussed case of impurity doping, the random field and, hence, this function are connected with all ionized impurities present in the sample.<sup>43</sup> It has been shown<sup>5-8</sup> that the autocorrelation function may capture the microscopic details not only of the geometry of the wire and the nature of the disorder but also of the many-body interaction in the 1DEG. On the other hand, our approach clearly works quite well with an arbitrary form of that function. Therefore, this enables us, to calculate the disorder effect on the energy spectrum of the interacting 1DEG in a QWR of any geometry and subjected to a smooth disorder of any origin.

#### IV. AUTOCORRELATION FUNCTIONS FOR A CYLINDRICAL SEMICONDUCTOR QWR

We shall now apply the foregoing theory to assess the influence on the DOS of 1DEG's in QWR's due to disorder arising from impurity doping and surface roughness, which are, in general, almost unavoidable in realistic wires. As our model of QWR's, we choose a circular cylinder and confine the motion of the electrons in the cylinder by an infinite potential barrier at its surface.<sup>5-8,48,49</sup> Accordingly, the wave functions of 1D subbands are proved to be expressed in terms of Bessel functions.<sup>5</sup> Moreover, at zero temperature almost all electrons are assumed to occupy the lowest 1D subband (extreme quantum limit), as shown experimentally.<sup>33,37</sup> As indicated just above, the theoretical analysis of the disorder effect is simply reduced to finding the autocorrelation function for the electron system to be treated.



### A. Impurity doping

We begin by examining random fluctuations in the impurity density in the sample. It is well known<sup>20,21</sup> that the random field created by all charged impurities is generally considered smooth at a high doping level. Moreover, the autocorrelation function of the total impurity field can be cast into the form<sup>43</sup>

$$W_{\text{ID}}(x-x') = n_I \int d^3 \mathbf{r}_i v(x-\mathbf{r}_i) v(x'-\mathbf{r}_i), \quad (24)$$

with  $n_I$  the 3D density of ionized impurities. Here  $v(x-\mathbf{r}_i)$  is the potential energy of an electron at  $\mathbf{r}=(x,0,0)$  due to a single impurity at  $\mathbf{r}_i=(x_i, \boldsymbol{\rho}_i)$ .

In the case in question, this potential obviously possesses the symmetry described by  $v(x-\mathbf{r}_i) = v(|x-x_i|, \boldsymbol{\rho}_i)$ . Therefore, the Fourier transform of Eq. (24) reads

$$W_{\text{ID}}(\mathbf{k}) = n_I \int d^2 \boldsymbol{\rho}_i v^2(\mathbf{k}, \boldsymbol{\rho}_i), \quad (25)$$

where  $v(\mathbf{k}, \boldsymbol{\rho}_i)$  is the Fourier transform in the  $x$  direction of the one-impurity potential.

The impurity potential is to be screened by interacting electrons in the 1DEG. This can be quantified by introducing a static dielectric function as

$$v(\mathbf{k}, \boldsymbol{\rho}_i) = \frac{v_{\text{ei}}(k, \boldsymbol{\rho}_i)}{\epsilon(k)}. \quad (26)$$

Here  $v_{\text{ei}}(k, \boldsymbol{\rho}_i)$  is the unscreened one-impurity potential, which is to be modified by a finite extension of the electron wave function  $\phi(\mathbf{r})$  in the  $y$  and  $z$  directions, i.e., weighted as<sup>5,14</sup>

$$v_{\text{ei}}(k, \boldsymbol{\rho}_i) = -Z \int d^2 \mathbf{r} |\phi(\mathbf{r})|^2 v(\boldsymbol{\rho}_i, \mathbf{r}, k), \quad (27)$$

with  $Z$  the charge of an ionized impurity in units of the electron charge  $e$ . The Coulomb potential figuring in Eq. (27) describes bare interaction between an electron at  $\mathbf{r}$  and an electron at  $\mathbf{r}'$ , given by<sup>14</sup>

$$v(\mathbf{r}, \mathbf{r}', k) = \frac{2e^2}{\epsilon_L} K_0(k|\mathbf{r}-\mathbf{r}'|), \quad (28)$$

with  $\epsilon_L$  the dielectric constant of the background lattice. In what follows,  $I_{n(x)}$  and  $K_{n(x)}$  are the  $n$ th-order modified Bessel functions of the first and second kind, respectively.<sup>47</sup>

As previously,<sup>48,49</sup> the electrons are, for simplicity, considered to be distributed with a constant density in the wire cross section. This implies that for the lowest subband we may take

$$|\phi(\mathbf{r})|^2 = (\pi R^2)^{-1} \theta(R-|\mathbf{r}|), \quad (29)$$

where  $R$  is the wire radius. The assumption of the uniform distribution of electrons may be a somewhat good approximation in the high-electron density limit because they repel each other.

Upon putting Eqs. (28) and (29) into Eq. (27), we obtain the following analytic form for the effective impurity potential:<sup>49</sup>

$$v_{\text{ei}}(k, \boldsymbol{\rho}_i) = -\frac{4Ze^2}{\epsilon_L} \frac{1}{\alpha^2} \begin{cases} 1 - \alpha K_1(\alpha) I_0(\delta_i) & \text{for } \delta_i \leq \alpha \\ \alpha I_1(\alpha) K_0(\delta_i) & \text{for } \delta_i \geq \alpha, \end{cases} \quad (30)$$

where  $\alpha = kR$  and  $\delta_i = k|\boldsymbol{\rho}_i|$ .

According to Eq. (25), the autocorrelation function for impurity doping depends on the geometry of the impurity system. Hereafter, the charged impurities are supposed to be randomly distributed in a cylindrical tube coaxial with the wire.

First, we are concerned with an infinitely thin impurity tube of radius  $\rho$ , integral (25) being trivial. The autocorrelation function depends on the position of the impurity system as follows.

(1)  $\rho \leq R$  and  $W_{\text{ID}} = W_{\text{MI}}$  (modulation doping inside the wire):

$$W_{\text{MI}}(\mathbf{k}) = \left( \frac{4Ze^2}{\epsilon_L} \right)^2 \frac{n_i}{\epsilon^2(k)} \frac{1}{\alpha^4} [1 - \alpha K_1(\alpha) I_0(\delta)]^2, \quad (31)$$

where  $n_i$  is the 1D impurity density along the tube axis, and  $\delta = k\rho$ .

(2)  $\rho > R$  and  $W_{\text{ID}} = W_{\text{MO}}$  (modulation doping outside the wire):

$$W_{\text{MO}}(\mathbf{k}) = \left( \frac{4Ze^2}{\epsilon_L} \right)^2 \frac{n_i}{\epsilon^2(k)} \frac{1}{\alpha^2} I_1^2(\alpha) K_0^2(\delta). \quad (32)$$

For an impurity tube of finite thickness with radii  $\rho_m$  and  $\rho_M$ , it is useful to distinguish between two limiting cases of interest.

(3)  $\rho_m = 0$ ,  $\rho_M = R$ , and  $W_{\text{ID}} = W_{\text{UI}}$  (uniform doping inside the wire):

$$W_{\text{UI}}(\mathbf{k}) = \left( \frac{4Ze^2}{\epsilon_L} \right)^2 \frac{n_i}{\epsilon^2(k)} \frac{1}{\alpha^4} \{1 - 4I_1(\alpha) K_1(\alpha) + \alpha^2 K_1^2(\alpha) [I_0^2(\alpha) - I_1^2(\alpha)]\}. \quad (33)$$

(4)  $\rho_m = R$ ,  $\rho_M > R$ , and  $W_{\text{ID}} = W_{\text{UO}}$  (uniform doping outside the wire):

$$W_{\text{UO}}(\mathbf{k}) = \left( \frac{4Ze^2}{\epsilon_L} \right)^2 \frac{n_i}{\epsilon^2(k)} \frac{1}{\alpha^4} I_1^2(\alpha) \{ \alpha^2 [K_1^2(\alpha) - K_0^2(\alpha)] - \delta_M^2 [K_1^2(\delta_M) - K_0^2(\delta_M)] \}, \quad (34)$$

where  $\delta_M = k\rho_M$ . The 1D impurity density in Eqs. (33) and (34) is fixed by the 3D one via  $n_i = \pi R^2 n_I$ .

If there exist several impurity species with charges  $Z_i$  and densities  $n_i$  in the sample, the product  $Z^2 n_i$  in Eqs. (31)–(34) is to be replaced with an effective impurity density, defined by

$$n_i^* = \sum_i Z_i^2 n_i. \quad (35)$$

### B. Surface roughness

Next we deal with random fluctuations in the wire radius that have been found to be important in very thin wires, e.g., made from  $\text{Al}_x\text{Ga}_{1-x}\text{As}/\text{GaAs}$ .<sup>17–19</sup> It is well known<sup>50</sup> that

the surface roughness in a QWR is characterized by the average size fluctuation  $\Delta$  and the correlation length  $\Lambda$  along the wire axis. Naively, one would argue that a decreasing  $\Delta$  or an increasing  $\Lambda$  corresponds to a smoother interface. A Gaussian-like decay of the wire radius fluctuations is usually assumed.

For the lowest subband, the autocorrelation function for surface roughness in a cylindrical QWR of radius  $R$  is then supplied by<sup>5-8</sup>

$$W_{SR}(\mathbf{k}) = (2.4)^4 \sqrt{\pi} \frac{\hbar^4 \Delta^2 \Lambda}{m^2 R^6} \frac{\exp(-\Lambda^2 k^2/4)}{\epsilon^2(k)}, \quad (36)$$

where  $\epsilon(k)$  allows for screening the surface roughness-induced field by the interacting 1DEG.

It is to be noted<sup>51</sup> that in case the 1DEG is affected simultaneously by both sources of disorder, the autocorrelation function is obviously additive if correlations between them are neglected, i.e.,

$$W(\mathbf{k}) = W_{ID}(\mathbf{k}) + W_{SR}(\mathbf{k}). \quad (37)$$

### C. RPA screening

It has been pointed out<sup>52</sup> that the disorder and screening effects are to self-consistently determine each other. Screening by interacting 1DEG's in QWR's is of great importance in determining disorder. In what follows, for the sake of numerical simplicity we neglect the influence of disorder on screening.<sup>13,49</sup> Then, within the random-phase approximation of the standard Fermi-liquid model, the static dielectric function for a 1DEG at zero temperature may be written as<sup>14,28-30</sup>

$$\epsilon(k) = 1 + \frac{2m}{\pi \hbar^2} \frac{v_{ee}(k)}{k} \ln \left| \frac{k + 2k_F}{k - 2k_F} \right|. \quad (38)$$

Here  $v_{ee}(k)$  denotes the Fourier transform in the  $x$  direction of the bare electron-electron interaction potential, and  $k_F$  is the Fermi wave vector fixed by the 1D carrier density  $n_e$  via  $k_F = (\pi/2)n_e$ .

The screening function (38) clearly exhibits a logarithmic singularity at  $k = 2k_F$ . It is well known that within the self-consistent Born approximation, the  $2k_F$  singularity of the function (38) leads to meaningless results at zero temperature for the 1D transport property<sup>52</sup> and the electronic 1D DOS,<sup>6</sup> so that the inclusion of the disorder effect in the calculation of screening is very important. However, this singularity presents no difficulty in our DOS calculation since all quantities of interest—the average potential  $\gamma$  and force  $F$ —are given in terms of the convergent  $k$  integrals as seen directly from Eqs. (18) and (19). The influence of disorder on screening is likely of less importance in the estimation of the field strength since this is significant mainly around the integrably singular point.<sup>14</sup>

The electron-electron interaction given by Eq. (28) is to be weighted with the wave function of the subband as<sup>5</sup>

$$v_{ee}(k) = \int d^2 \mathbf{r} \int d^2 \mathbf{r}' |\phi(\mathbf{r})|^2 |\phi(\mathbf{r}')|^2 v(\mathbf{r}, \mathbf{r}', k). \quad (39)$$

Inserting Eqs. (28) and (29) into Eq. (39) yields the effective electron-electron interaction in analytic form.<sup>49</sup>

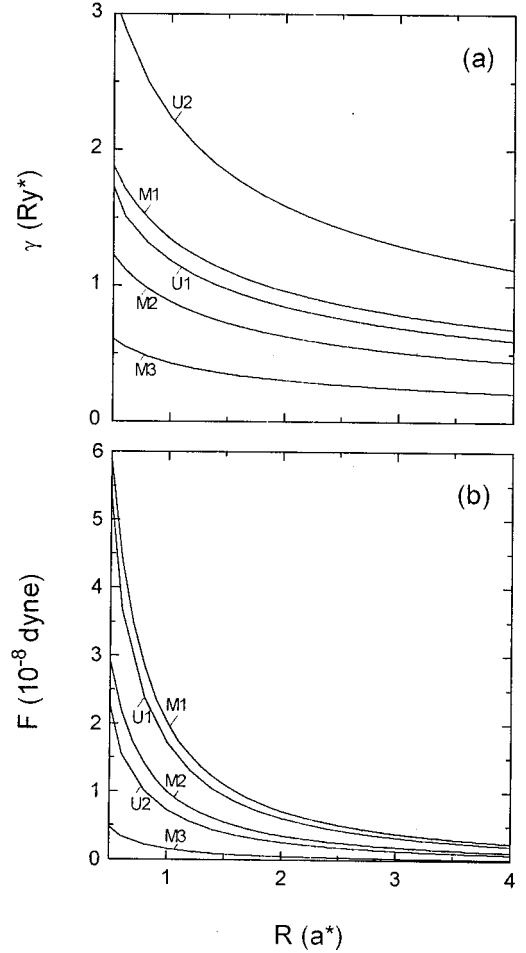


FIG. 1. rms of the (a) potential  $\gamma$  and (b) force  $F$  for impurity doping vs wire radius  $R$  under density  $n_i = n_e = 10^6 \text{ cm}^{-1}$ . The labels  $M1$ ,  $M2$ , and  $M3$  refer to modulation doping with various impurity positions  $\rho = 0, R$ , and  $2R$ .  $U1$  and  $U2$  refer to inside and outside uniform doping with  $\rho_m = 0$ ,  $\rho_m = R$  and  $\rho_m = R$ ,  $\rho_m = 6R$ , respectively.

$$v_{ee}(k) = \frac{4e^2}{\epsilon_L} \frac{1}{\alpha^2} [1 - 2I_1(\alpha)K_1(\alpha)] \quad (40)$$

( $\alpha = kR$ ).

## V. RESULTS AND DISCUSSIONS

To illustrate the theory developed in the preceding sections, we have carried out numerical calculations for cylindrical QWR's made of  $n$ -type GaAs at zero temperature, whose conduction subband is considered. The material parameters are the effective mass  $m = 0.067m_e$  and the dielectric constant  $\epsilon_L = 12.9$ . However, our results are more general. This is because that the natural scales for the length, the energy, and the 1D DOS are atomic units: the effective Bohr radius  $a^* = \epsilon_L \hbar^2 / me^2$ , the effective Rydberg  $\text{Ry}^* = me^4 / 2\epsilon_L^2 \hbar^2$ , and  $\rho^* = 1/\text{Ry}^* a^*$ , respectively. For GaAs wires, we have  $a^* = 100 \text{ \AA}$ ,  $\text{Ry}^* = 5.6 \text{ meV}$ , and  $\rho^* = 1.79 \times 10^5 \text{ meV}^{-1} \text{ cm}^{-1}$ . The DOS of the disordered 1DEG in a QWR is determined by Eq. (22), where the average potential

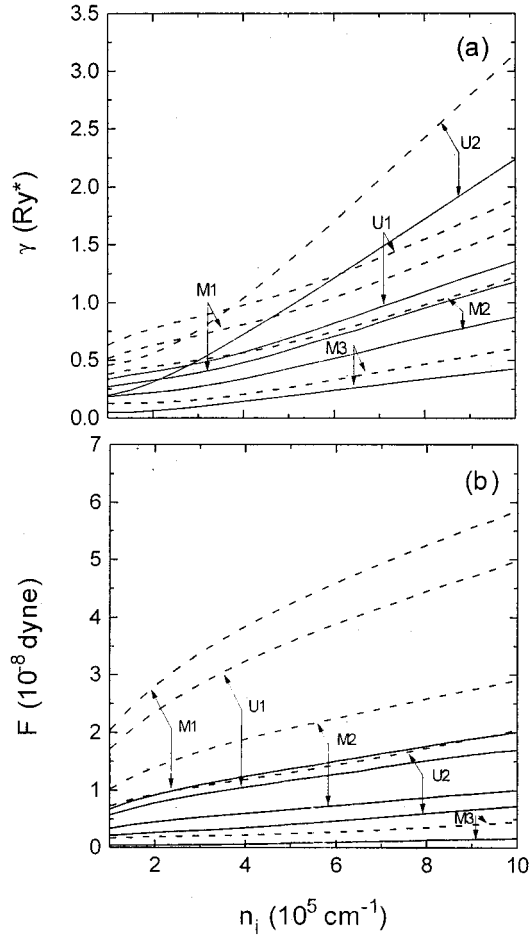


FIG. 2. rms of the (a) potential  $\gamma$  and (b) force  $F$  for impurity doping vs density  $n_i$  ( $n_i = n_e$ ) under different wire radii  $R = a^*/2$  (dashed lines) and  $a^*$  (solid lines). The labels are the same as in Fig. 1.

$\gamma$  and force  $F$  of the random field are given by Eqs. (18) and (19) in terms of its autocorrelation function.

### A. Impurity doping

First, we evaluate the disorder effect due to impurity doping with the autocorrelation function given by Eqs. (31) and (32) for modulation doping, and Eqs. (33) and (34) for uniform doping. From these it follows that the random parameters  $\gamma$  and  $F$  depend on the radius of the electron wire  $R$  and those of the impurity tube  $\rho_m$  and  $\rho_M$  as well as their densities  $n_i$  and  $n_e$ . Hereafter, the case of  $n_i = n_e$  is discussed.

In Fig. 1 the rms of the potential  $\gamma$  and force  $F$  for impurity doping are plotted vs wire radius  $R$  under impurity density  $n_i = 10^6 \text{ cm}^{-3}$ : modulation doping with various impurity positions  $\rho = 0$ ,  $R$ , and  $2R$ ; and inside and outside doping with  $\rho_m = 0$ ,  $\rho_M = R$  and  $\rho_m = R$ ,  $\rho_M = 6R$ , respectively. In Fig. 2 the random parameters  $\gamma$  and  $F$  are plotted vs impurity density  $n_i$  for different wire radii  $R = a^*/2$  and  $a^*$ . In Fig. 3 the DOS  $\rho(E)$  is plotted vs energy for the IDEG subjected to impurity doping with density  $n_i = 10^6 \text{ cm}^{-3}$  under different wire radii  $R = a^*/2$ ,  $a^*$ , and  $2a^*$ . The DOS of the ideal IDEG is depicted according to Eq. (23). In Fig. 4 the DOS  $\rho(E)$  is plotted vs energy for the IDEG subjected to outside

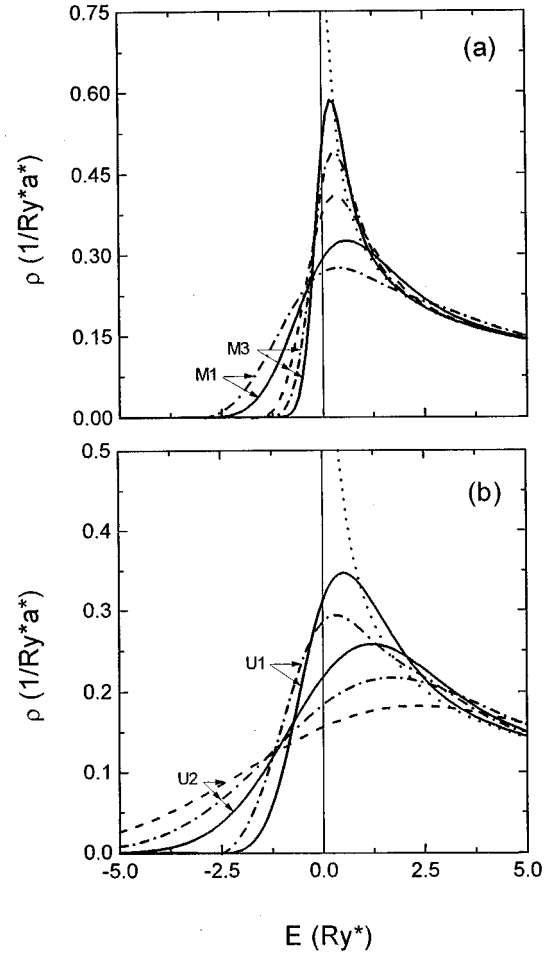


FIG. 3. DOS  $\rho(E)$  in units of  $\rho^*$  vs energy for the IDEG subjected to impurity doping with density  $n_i = n_e = 10^6 \text{ cm}^{-3}$  under different wire radii  $R = a^*/2$  (dashed lines),  $a^*$  (dash-dotted lines), and  $2a^*$  (solid lines). The DOS is plotted for (a) modulation doping  $M1$  and  $M3$ , and (b) uniform doping  $U1$  and  $U2$ . The labels are the same as in Fig. 1. The dotted line represents the DOS of the ideal IDEG.

doping with wire radius  $R = 4a^*$ , under various impurity densities  $n_i = 10^5$ ,  $5 \times 10^5$ , and  $10^6 \text{ cm}^{-3}$ .

It should be mentioned that we cannot employ Eq. (22) to calculate the disorder effects on the 1D DOS due to inside and outside doping with  $n_i \leq 5 \times 10^5 \text{ cm}^{-3}$  and  $R \leq 2a^*$ , and inside doping with  $n_i \leq 10^6 \text{ cm}^{-3}$  and  $R \leq a^*/2$ , since in these cases the semiclassical condition (8) is broken.

### B. Surface roughness

Next we assess the disorder effect from surface roughness with the autocorrelation function (36). It is obvious that the surface roughness parameters depend on the wire fabrication technique. For GaAs the average size fluctuation  $\Delta$  is assumed ranged from 3 to 20 Å, and the correlation length  $\Lambda$  from 20 to 200 Å.<sup>10</sup> Small values of  $\Delta$  correspond to fabrication by molecular-beam epitaxy<sup>53,54</sup> and the large ones to fabrication, e.g., by electron-beam lithography and wet chemical etching.<sup>55</sup>

In Fig. 5 the rms of the potential  $\gamma$  and force  $F$  are plotted vs wire radius  $R$  under correlation length  $\Lambda = a^*$ , various

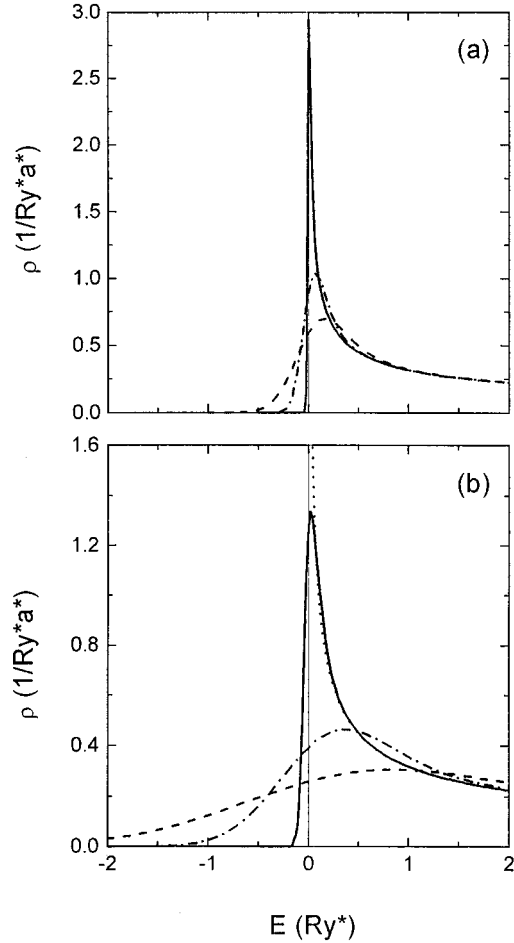


FIG. 4. DOS  $\rho(E)$  in units of  $\rho^*$  vs energy for the 1DEG subjected to outside impurity doping with wire radius  $R=4a^*$  under various densities  $n_i=n_e=10^5 \text{ cm}^{-1}$  (solid lines),  $5 \times 10^5 \text{ cm}^{-1}$  (dash-dotted lines), and  $10^6 \text{ cm}^{-1}$  (dashed lines). The DOS is plotted for (a) modulation doping  $M3$  and (b) uniform doping  $U2$ . The labels are the same as in Fig. 1.

radius fluctuations  $\Delta=3, 10, \text{ and } 20 \text{ \AA}$ , and different electron densities  $n_e=10^5$  and  $10^6 \text{ cm}^{-1}$ . In Fig. 6 the random parameters  $\gamma$  and  $F$  are plotted vs correlation length  $\Lambda$  under wire radius  $R=a^*$ , various radius fluctuations  $\Delta=3, 10, \text{ and } 20 \text{ \AA}$ , and different electron densities  $n_e=10^5$  and  $10^6 \text{ cm}^{-1}$ . In Fig. 7 the DOS  $\rho(E)$  is plotted vs energy for the 1DEG subjected to surface roughness with correlation length  $\Lambda=a^*$  and various radius fluctuations  $\Delta=3, 10, \text{ and } 20 \text{ \AA}$  under electron density  $n_e=10^6 \text{ cm}^{-1}$  and different wire radii  $R=a^*/2$  and  $a^*$ .

Finally, Fig. 8 displays the DOS  $\rho(E)$  of the 1DEG subjected to both sources of disorder: impurity doping with density  $n_i=10^6 \text{ cm}^{-1}$  and surface roughness with radius fluctuation  $\Delta=10 \text{ \AA}$  and correlation length  $\Lambda=a^*$ . The DOS using Eq. (37), is plotted under different wire radii:  $R=a^*/2$  for combining the effects of outside doping and surface roughness, and  $R=a^*$  for combining the ones of inside doping and surface roughness. As in the 2D case,<sup>56</sup> the resulting effect is found not equal to merely the sum of the two effects, each one being treated separately.

It is worth noting that the average potential is seen to be small compared with the energy separation between the first

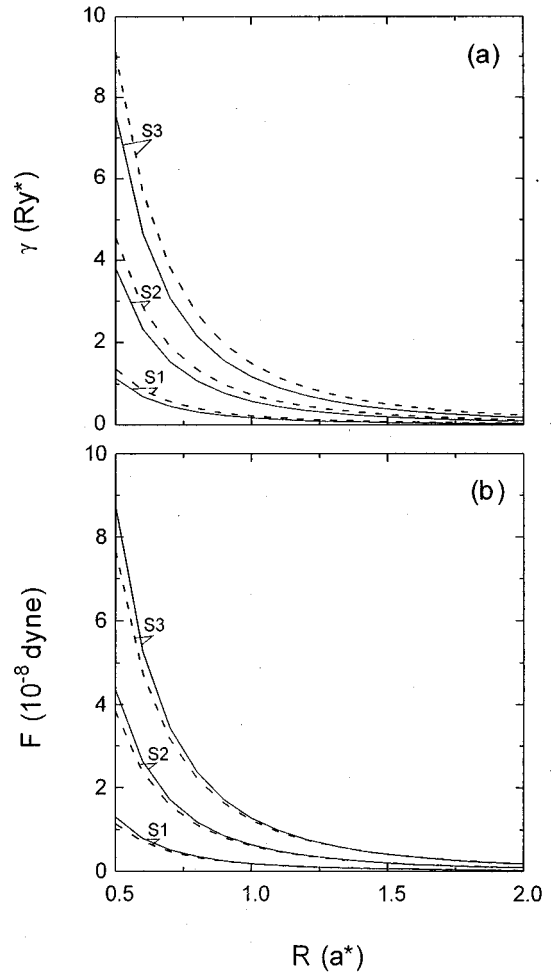


FIG. 5. rms of the (a) potential  $\gamma$  and (b) force  $F$  for surface roughness vs wire radius  $R$  under correlation length  $\Lambda=a^*$ , and different electron densities  $n_e=10^5 \text{ cm}^{-1}$  (solid lines) and  $10^6 \text{ cm}^{-1}$  (dashed lines). The labels  $S1, S2, \text{ and } S3$  correspond to surface roughness with various size fluctuations  $\Delta=3, 10, \text{ and } 20 \text{ \AA}$ , respectively.

and second subbands given by<sup>57</sup>  $E_1-E_0=8.9(a^*/R)^2 \text{ Ry}^*$ , which warrants the one-subband approximation used.

### C. Conclusions

From the curves thus obtained we may draw the following results.

(i) Figures 1 and 5 indicate the strength of the random fields connected with impurity doping and surface roughness in thin QWR's is enhanced rapidly when reducing the wire size. For  $R \leq a^*/2$  surface roughness (especially with large  $\Delta$ ) is observed to overwhelm impurity doping. But for  $R \geq 2a^*$  the former is negligible, whereas the latter becomes dominant. These disorder sources compete for  $R \approx a^*$ .

(ii) It follows, as expected, from Fig. 2 that the strength of the total impurity field increases when elevating the doping level  $n_i$ .

(iii) Figures 5 and 6 reveal the strength of the surface roughness field exhibits a linear enhancement with increasing the radius fluctuation  $\Delta$ ; see Eq. (36). Moreover, the random field is weakened when increasing the correlation



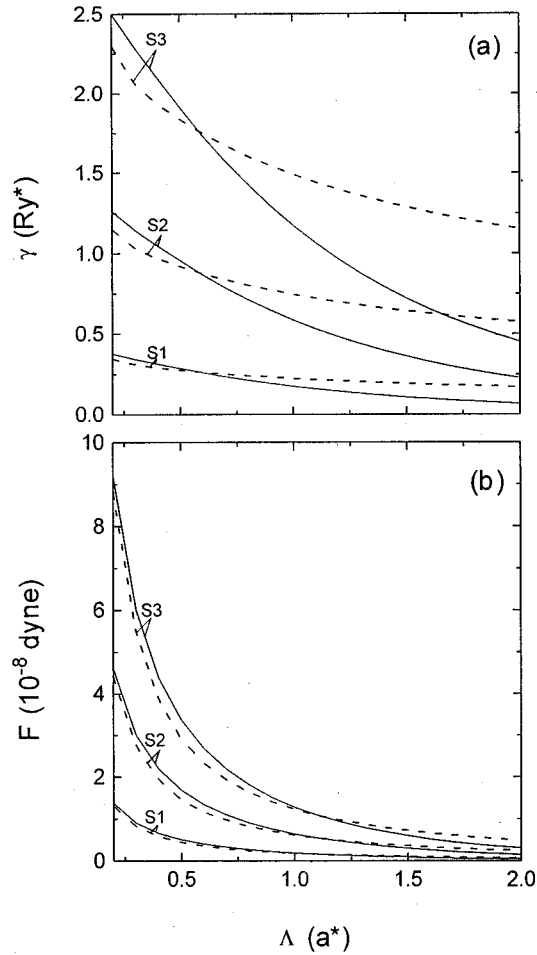


FIG. 6. rms of the (a) potential  $\gamma$  and (b) force  $F$  for surface roughness vs correlation length  $\Lambda$  for wire radius  $R=a^*$ , under different electron densities  $n_e=10^5 \text{ cm}^{-1}$  (solid lines) and  $10^6 \text{ cm}^{-1}$  (dashed lines). The labels are the same as in Fig. 5.

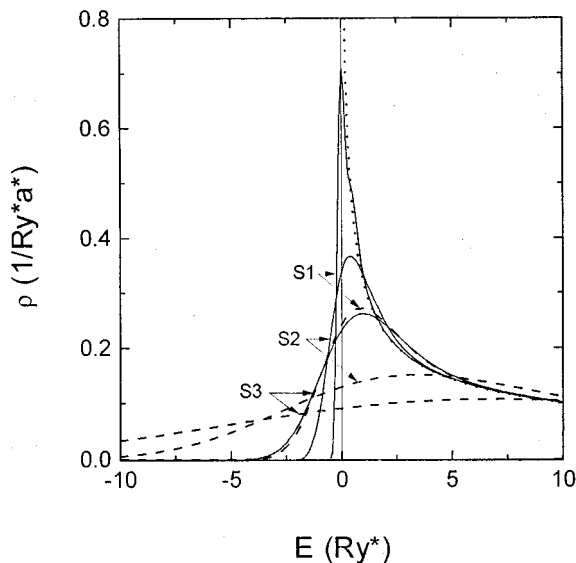


FIG. 7. DOS  $\rho(E)$  in units of  $\rho^*$  vs energy for the 1DEG subjected to surface roughness with correlation length  $\Lambda=a^*$  under different wire radii  $R=a^*/2$  (dashed lines) and  $a^*$  (solid lines), and electron density  $n_e=10^6 \text{ cm}^{-1}$ . The labels are the same as in Fig. 5.

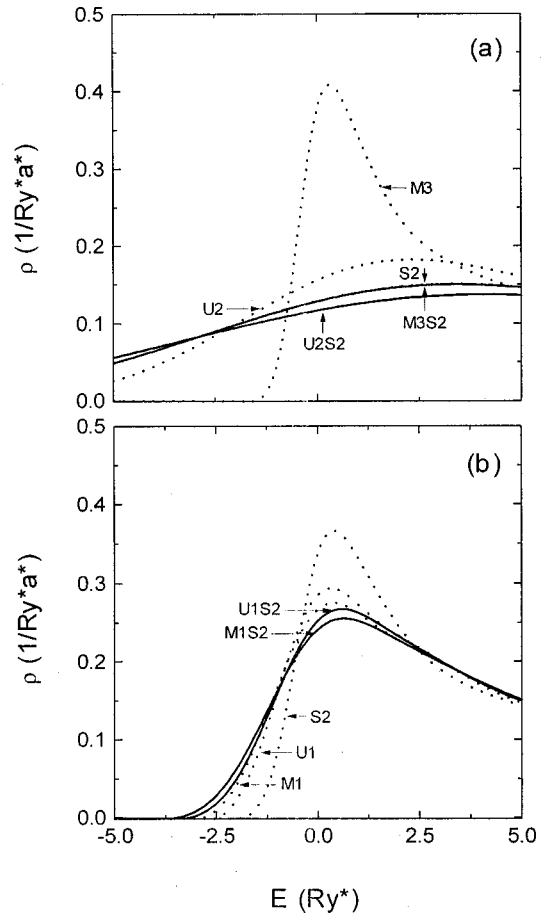


FIG. 8. DOS  $\rho(E)$  in units of  $\rho^*$  vs energy for the 1DEG subjected to both impurity doping with density  $n_i=n_e=10^6 \text{ cm}^{-1}$  and surface roughness with radius fluctuation  $\Delta=10 \text{ \AA}$  and correlation length  $\Lambda=a^*$ . The DOS is plotted under different wire radii: (a)  $R=a^*/2$  for outside doping  $M3$  and  $U2$  and surface roughness  $S2$ , and the combined effect is marked by  $M3S2$  and  $U2S2$ . (b)  $R=a^*$  for inside doping  $M1$  and  $U1$  and surface roughness  $S2$ , and the combined effect  $M1S2$  and  $U1S2$ . The labels are the same as in Figs. 1 and 5.

length  $\Lambda$ . The surface roughness potential drops with  $\Lambda$  rather rapidly for small  $R$  and large  $\Delta$ , but slowly for large  $R$ .

(iv) An examination of Figs. 3, 4, 7, and 8 shows the squared-root singularity of the DOS of the ideal 1DEG is destroyed by disorder into a finite peak. The disorder not only dramatically reduces the height of the peak and pushes it up toward higher energies, but also gives rise to a band tail (of localized states) extending deep below the subband edge. The electronic energy spectrum of the 1DEG is found to be considerably modified in a region around the subband edge and of the order of the average potential  $\gamma$ , as quoted previously. The DOS of the ideal and disordered 1DEG's are asymptotically equal. This means the disorder effect is negligible at very high energies.

It is worthy to recall that the DOS tail ( $E<0$ ) cannot be provided within the 1D semiclassical theory due to Takeshima,<sup>12</sup> nor within the 1D multiple scattering theory of Ref. 16. Further, in comparison with the 2D and 3D cases,<sup>25,43</sup> the modification of the 1D DOS around the subband edge is much more drastic. The reason for this is that in

the 1D case the singularity of the DOS at the subband edge and the disorder interaction are both stronger, the screening by the IDEG being weaker.

(v) The characteristics of the DOS (its peak and tail) are seen to depend on the wire size. Figures 3 and 7 indicate that the DOS peak is lowered, and the DOS tail is larger and more extended below the subband edge when reducing the wire radius. This means that the thinner the wire, the stronger the disorder effect becomes.

(vi) Figures 4 and 7 reveal that the DOS peak is lowered and the DOS tail is larger and more extended far below the subband edge when increasing the doping level  $n_i$  or the size fluctuation  $\Delta$ .

(vii) As in the 2D and 3D cases, the disorder-induced shift of the Fermi level of the IDEG is found to be small, which is in contrast to the earlier result.<sup>12</sup> Indeed, at density  $n_e = n_i = 10^6 \text{ cm}^{-3}$  the Fermi level of the ideal IDEG is equal to  $E_F^{(0)} = 2.50 \text{ Ry}^*$ . The Fermi level of the disordered IDEG in a wire of radius  $R = a^*$ , using Eq. (22), is estimated to be  $E_F = 2.70$  and  $2.94 \text{ Ry}^*$  under inside modulation doping with  $\rho = 0$  and outside uniform doping with  $\rho_M = 6R$ , respectively; and  $E_F = 2.54 \text{ Ry}^*$  under surface roughness with  $\Lambda = a^*$  and  $\Delta = 10 \text{ \AA}$ . This is interpreted as follows. As quoted above, the 1D DOS, on the one hand, is reduced appreciably in the intrasubband near the subband edge; on the other hand, it is remarkably enhanced on the tail far below the subband edge, the Fermi level being slightly shifted.

## VI. SUMMARY

In this paper we have achieved a simple analytic expression [Eq. (22)] for the DOS of disordered quasi-1DEG's in semiconductor QWR's, in which the input function for disorder interaction is the autocorrelation function in wavevector space. This enables us, to calculate the effect on the

1D DOS due to a source of disorder other than impurity doping, e.g., surface roughness, and that due to many-body screening caused by realistic IDEG's in QWR's. In particular, it is possible to go beyond the random-phase approximation, including the local-field correction (electron exchange and correlation) into the DOS calculation.

In our model of cylindrical QWR's with an infinite potential barrier, the cylindrical symmetry is used. As indicated previously,<sup>5,49</sup> this could not alter the order of magnitude of the disorder effects, but does enable the input function to be given in analytic form for various disorder sources. Therefore, a numerical calculation of the 1D DOS as well as the observable properties of realistic QWR's relative to the DOS, e.g., optical absorption, presents no difficulty.

It should be kept in mind that our semiclassical approach describes a smooth random field which obeys inequality (8) valid for disorder of any origin. The disorder is clearly connected only with long-range fluctuations in the disorder potential (e.g., due to heavy doping and slowly varying surface roughness) and modifies the 1D DOS in the high-energy region (around the subband edge). For disorder associated with short-range potential fluctuations (e.g., doping inside a very thin QWR or at a lower doping level, and alloy disorder with a  $\delta$  potential), the theory is inapplicable. Then, also to include the short-range potential fluctuations and, hence, the low-energy region (deep tail), in a forthcoming paper we will supply a path-integral approach based on a cumulant approximation, modifying the method developed recently by Quang and Tung<sup>58</sup> for 2D electron systems.

Owing to the absence of detailed experimental information about the electronic energy spectrum of disordered QWR's, a quantitative comparison with experiments is presently impossible. We hope that our analytic results stimulate theoretical investigations and help to clarify future experimental results.

<sup>1</sup>C. Weisbuch and B. Vinter, *Quantum Semiconductor Structures* (Academic, San Diego, 1991).

<sup>2</sup>H. Sakaki, *J. Appl. Phys.* **19**, L735 (1980); *J. Vac. Sci. Technol.* **19**, 148 (1981).

<sup>3</sup>Y. Arakawa and A. Yariv, *IEEE J. Quantum Electron.* **22**, 1887 (1986).

<sup>4</sup>S. Schmitt-Rink, D. A. B. Miller, and D. A. Chemla, *Phys. Rev. B* **35**, 8113 (1987).

<sup>5</sup>A. Gold and A. Ghazali, *Phys. Rev. B* **41**, 7626 (1990).

<sup>6</sup>A. Gold, *Phys. Rev. B* **46**, 2339 (1992).

<sup>7</sup>B. Tanatar and A. Gold, *Phys. Rev. B* **52**, 1996 (1995).

<sup>8</sup>J. S. Thakur and D. Neilson, *Phys. Rev. B* **56**, 4679 (1997); **56**, 7485 (1997).

<sup>9</sup>J. Motohisa and H. Sakaki, *Appl. Phys. Lett.* **60**, 1315 (1992).

<sup>10</sup>I. Vurgaftman and J. R. Meyer, *Phys. Rev. B* **55**, 4494 (1997).

<sup>11</sup>P. K. Basu and C. K. Sarkar, *Surf. Sci.* **174**, 454 (1986).

<sup>12</sup>M. Takeshima, *Phys. Rev. B* **33**, 7047 (1986).

<sup>13</sup>A. Ghazali, A. Gold, and J. Serre, *Semicond. Sci. Technol.* **8**, 1912 (1993).

<sup>14</sup>S. Das Sarma and W. Y. Lai, *Phys. Rev. B* **32**, 1401 (1985).

<sup>15</sup>S. Das Sarma and X. C. Xie, *Phys. Rev. B* **35**, 9875 (1987).

<sup>16</sup>E. A. de Andrada e Silva, I. C. da Cunha Lima, and A. Ferreira da

Silva, *Phys. Rev. B* **37**, 8537 (1988).

<sup>17</sup>T. J. Thornton, M. L. Roukes, A. Scherer, and B. P. Van de Gaag, *Phys. Rev. Lett.* **63**, 2128 (1989).

<sup>18</sup>S. Block, M. Suhrke, S. Wilke, A. Menschig, H. Schweizer, and D. Grützmacher, *Phys. Rev. B* **47**, 6524 (1993).

<sup>19</sup>M. Notomi, M. Okamoto, and T. Tamamura, *J. Appl. Phys.* **75**, 4161 (1994).

<sup>20</sup>E. O. Kane, *Phys. Rev.* **131**, 79 (1963).

<sup>21</sup>V. L. Bonch-Bruевич, *Fiz. Tverd. Tela (Leningrad)* **4**, 2660 (1962) [*Sov. Phys. Solid State* **4**, 1953 (1963)].

<sup>22</sup>J. A. Reyes and M. del Castillo-Mussot, *Phys. Rev. B* **57**, 9869 (1998).

<sup>23</sup>J. R. Klauder, *Ann. Phys. (N.Y.)* **14**, 43 (1961).

<sup>24</sup>T. Matsubara and Y. Toyozawa, *Prog. Theor. Phys.* **26**, 739 (1961).

<sup>25</sup>D. N. Quang and N. H. Tung, *Phys. Status Solidi B* **207**, 111 (1998).

<sup>26</sup>See, e.g., P. A. Lee and T. V. Ramakrishnan, *Rev. Mod. Phys.* **57**, 287 (1985).

<sup>27</sup>See, e.g., G. D. Mahan, *Many-Particle Physics*, 2nd ed. (Plenum, New York, 1990).

<sup>28</sup>B. Y.-K. Hu and S. Das Sarma, *Phys. Rev. Lett.* **68**, 1750 (1992); *Phys. Rev. B* **48**, 5469 (1993).

- <sup>29</sup>Q. P. Li, S. Das Sarma, and R. Joynt, Phys. Rev. B **45**, 13 713 (1992).
- <sup>30</sup>S. Das Sarma and E. H. Hwang, Phys. Rev. B **54**, 1936 (1996).
- <sup>31</sup>D. Z. Liu and S. Das Sarma, Phys. Rev. B **51**, 13 821 (1995).
- <sup>32</sup>A. S. Plaut, H. Lage, P. Grambow, D. Heitmann, K. von Klitzing, and K. Ploog, Phys. Rev. Lett. **67**, 1642 (1991).
- <sup>33</sup>A. R. Gōni, A. Pinczuk, J. S. Weiner, J. M. Calleja, B. S. Dennis, L. N. Pfeiffer, and K. W. West, Phys. Rev. Lett. **67**, 3298 (1991).
- <sup>34</sup>J. M. Calleja, A. R. Gōni, B. S. Dennis, J. S. Weiner, A. Pinczuk, S. Schmidt-Rink, L. N. Pfeiffer, K. W. West, J. F. Müller, and A. E. Ruckenstein, Solid State Commun. **79**, 991 (1991).
- <sup>35</sup>R. Cingolani, R. Rinaldi, M. Ferrara, G. C. La Rocca, H. Lage, D. Heitmann, K. Ploog, and H. Kalt, Phys. Rev. B **48**, 14 331 (1993).
- <sup>36</sup>A. R. Gōni, A. Pinczuk, J. S. Weiner, B. S. Dennis, L. N. Pfeiffer, and K. W. West, Phys. Rev. Lett. **70**, 1151 (1993).
- <sup>37</sup>A. Schmeller, A. R. Gōni, A. Pinczuk, J. S. Weiner, J. M. Calleja, B. S. Dennis, L. N. Pfeiffer, and K. W. West, Phys. Rev. B **49**, 14 778 (1994).
- <sup>38</sup>A. Newton Borges, S. A. Leão, and O. Hipólito, Phys. Rev. B **55**, 4680 (1997).
- <sup>39</sup>E. H. Hwang and S. Das Sarma, Phys. Rev. B **58**, R1738 (1998).
- <sup>40</sup>M. F. Lin and K. W.-K. Shung, Phys. Rev. B **47**, 6617 (1993).
- <sup>41</sup>O. Sato, Y. Tanaka, M. Kobayashi, and A. Hasegawa, Phys. Rev. B **48**, 1947 (1993).
- <sup>42</sup>B. Tanatar, Phys. Rev. B **55**, 1361 (1997).
- <sup>43</sup>P. Van Mieghem, Rev. Mod. Phys. **64**, 755 (1992).
- <sup>44</sup>V. L. Bonch-Bruевич, A. G. Mironov, and I. P. Zviagin, Riv. Nuovo Cimento **3**, 321 (1973).
- <sup>45</sup>V. L. Bonch-Bruевич, R. Enderlein, B. Esser, R. Keiper, A. G. Mironov, and I. P. Zviagin, *Einführung in die Elektronentheorie ungeordneter Halbleiter* (VEB Deutscher Verlag der Wissenschaften, Berlin, 1984).
- <sup>46</sup>D. N. Quang, N. N. Dat, and D. V. An, J. Phys. Soc. Jpn. **66**, 140 (1997).
- <sup>47</sup>I. S. Gradshteyn and I. M. Ryzhik, *Table of Integrals, Series, and Products*, 4th ed. (Academic, New York, 1980).
- <sup>48</sup>L. Lee and H. P. Spector, J. Appl. Phys. **57**, 366 (1985).
- <sup>49</sup>G. Fishman, Phys. Rev. B **34**, 2394 (1986).
- <sup>50</sup>T. Ando, A. B. Fowler, and F. Stern, Rev. Mod. Phys. **54**, 437 (1982).
- <sup>51</sup>A. Gold, Phys. Rev. B **35**, 723 (1987).
- <sup>52</sup>B. Y.-K. Hu and S. Das Sarma, Phys. Rev. B **48**, 14 388 (1993).
- <sup>53</sup>H. Sakaki, T. Noda, K. Hirakawa, M. Tanaka, and T. Matsusue, Appl. Phys. Lett. **54**, 1934 (1987).
- <sup>54</sup>R. Göttinger, A. Gold, G. Abstreiter, G. Weimann, and W. Schlapp, Europhys. Lett. **6**, 183 (1988).
- <sup>55</sup>P. Ils, A. Forchel, K. H. Wang, Ph. Pagnod-Rossiaux, and L. Goldstein, Phys. Rev. B **50**, 11 746 (1994).
- <sup>56</sup>J. Serre, A. Ghazali, and A. Gold, Phys. Rev. B **39**, 8499 (1989).
- <sup>57</sup>A. Gold and A. Ghazali, Phys. Rev. B **41**, 8318 (1990).
- <sup>58</sup>D. N. Quang and N. H. Tung, Phys. Status Solidi B **209**, 375 (1998).